EasyChair Preprint

№ 8100

Rainbow Smart Metamaterial to Improve Flexural Wave Isolation and Vibration Attenuation of a Beam

Braion B. Moura and Marcela R. Machado

EasyChair preprints are intended for rapid dissemination of research results and are integrated with the rest of EasyChair.

May 28, 2022

Rainbow smart metamaterial to improve flexural wave isolation and vibration attenuation of a beam *

Braion B. Moura[1 [0000−0003−0314−730X]] and Marcela R. Machado[1 [0000−0002−7488−7201]]

Department of Mechanical Engineering, University of Brasilia, 70910-900, Brasília, Brazil. braionbarbosa@gmail.com

Abstract. This article analyzes wave propagation isolation and vibration attenuation strategies of a beam coupled to piezoelectric sensors periodically arranged in a given frequency band. Each piezo sensor is connected to a resonant shunt circuit. The influence on the attenuation band is due to a tunable shunt impedance associated with the corresponding piezo. Hence, the piezo's resonate at different and neighbouring frequencies creates a tunable rainbow trap that can attenuate the energy within a bandgap characteristic. The smart metastructure is modelled by means of the spectral element method, which is a highly accurate method with a low computational cost. Flexural wave propagation is obtained using the Transfer Matrix Method with the scatter diagram plot. Results show the effect of broadband vibrations' attenuation and propagating waves isolation. Moreover, the spectral range over which attenuation is achieved with the rainbow arrangements is on average wider than the usual metamaterials configurations.

Keywords: Rainbow metamaterial · Smart metastructure · Spectral element method · Transfer matrix method.

1 Introduction

The smart materials, metamaterials and metastructure are structures increasingly applied in advanced multi-physics systems. Piezoelectric materials (piezo) coupled to beams, bars and plates are a structural example of smart materials and metamaterials capable of exerting vibrational control and wave propagation. Such control depends on the operational configuration of the piezos that can convert energy from the mechanical to electrical domain and vice versa, that is, direct piezoelectric effect when the piezo converts the mechanical stress into an electric field, and reverse piezoelectric effect when the piezo converts the electric field into mechanical stress [11]. Each operational configuration allows the evolution of these smart materials and metamaterials, where the potential

* Supported by organization FAPDF.

for on-demand ownership modulation can be achieved by passive, active or hybrid control [3, 8]. Active vibration control techniques are related to the reverse piezoelectric effect, where they use an electrical energy source to increase the mechanical energy needed by the system. Unlike active techniques, passive vibration control techniques use the direct piezoelectric effect, making changes in the electrical energy generated by the piezo to promote a specific dynamic property in the structure, without relying on an external source of electrical energy [6]. Hybrid vibration controls combine both active and passive control techniques.

In the literature, several studies address the use of passive vibrational control with piezos connected to external circuits composed of passive components such as resistors, inductors and capacitors [5]. These circuits, known by the term shunt, began to be explored by Foward (1979) with the aim of inducing vibrations. Later, Uchino and Ishii (1988) explored the direct piezoelectric effect, dissipating the resulting electrical energy through an external resistance. Thus, it was noticed that a significant variation in the structure's damping factor occurs when the value of the external resistance is changed. Hagood and Flotow (1988) continued their study of the resistive shunt circuit, but added the inductive element and realized the ability to adjust the attenuation effect in frequency, similar to a dynamic vibration absorber. From there, other works explore various combinations of circuits with resistive-inductive elements applied to vibrational control, and these circuits became known by the term resonant shunt circuits [7, 15, 1, 17, 13].

The application of passive control with the resonant shunt circuit is commonly performed identically and periodically along a structure. However, some works are using the resonant shunt circuit with the coupling configuration of 7 piezos tuned at different frequencies, but close to each other. This coupling configuration is called a rainbow trap and can provide attenuation in a given frequency band [2, 16, 9]. In this context, the present work aims to explore the Frequency Response Function (FRF) and the Scatter Diagram (DD) of a beam subjected to a vibrational control with resonant shunt in the rainbow trap configuration. With this, we intend to investigate the influence that each piezo causes on the attenuation width. For this, numerical models are developed based on SEM to perform accurate and computationally efficient analyses, without the need for large discretizations. Furthermore, the Transfer Matrix Method (TMM) is used to estimate the DD of the structure.

2 Smart Material Theory Background

The SEM is considered a very efficient method for representing different types of geometries, boundary conditions and materials. Part of the efficiency of this method is due to the fact that the shape functions of the elements are obtained from the analytical solution of the governing differential equations and the solution of the dynamical system written in the domain frequency [4]. The SEM can represent the smart beam with the subdivision of beam (B) and beam-piezo-

shunt (BPS) elements, as shown in Figure 1. Each element is composed of two nodes and each node has three degrees of freedom based on the Euler-Bernoulli theory [10].

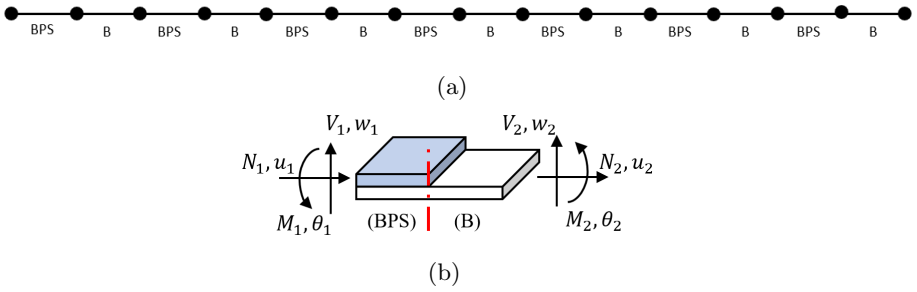

Fig. 1: Representation: a) Spectral model of the structure; b) Free-body diagram.

For the beam element (B), Doyle (1997) reports that through the nodal relations of force and displacement it is possible to express the spectral stiffness matrix $\mathbf{S}_B(\omega)$ for the Euler-Bernoulli beam element. Similarly, Lee (2000) reports how to obtain the spectral stiffness matrix $\mathbf{S}_{BP}(\omega)$ for the beam element with a uniformly coupled piezo layer. However, the mathematical representation of the beam-piezo element connected to a resonant shunt circuit (BPS) is given by the following equation of motion

$$\begin{aligned} &EIw'''' + \rho A\ddot{w} + cA\dot{w} + \Gamma V = -\alpha\ddot{u}_b' + \beta u''' + \gamma\ddot{w}'' + c_1\dot{w}'' - c_4\dot{u}_b' + Fw'' \\ &+ p(x,t) \\ &EAu_b'' - \rho A\ddot{u}_b - cA\dot{u}_b + \Gamma V = -\alpha\ddot{w}' + \beta w''' - c_4\dot{w}' - \Gamma(x,t) \\ &E\tau\dot{x} + C_P^T\dot{V} = I_c(x,t) \end{aligned} \tag{1}$$

where

$$\begin{aligned} \alpha &= (1/2)\rho_p A_p h, & EI &= E_b I_b + E_p I_p + (1/4)\, E_p A_p h^2, & c_1 &= (1/4) c_p A_p h^2, \\ \beta &= (1/2) E_p A_p h, & EA &= E_b A_b + E_p A_p, & c_4 &= (1/2) c_p A_p h, \\ \gamma &= (1/4)\rho_p A_p h^2, & \rho A &= \rho_b A_b + \rho_p A_p, & cA &= c_b A_b + c_p A_p \end{aligned}$$

where $(\prime)$ denotes space derivative, $(\dot{})$ denotes time derivative, and viscous damping coefficients is presented by c, and $p(x,t)$ and $\tau(x,t)$ are the external forces applied along the beam. The E, ρ, A and I are Young's modulus, mass density, transverse area and moment of inertia, respectively. Furthermore, I_c is the current, V is the voltage, C_P^T is the piezoelectric capacitance, Γ is the coupling term.

The global stochastic electromechanical equation of motion coupling the shunt circuit to the piezoelectric component is defined in terms of the spectral stiffness matrix as [12],

$$\begin{aligned} \mathbf{S}_{BP}(\omega)\mathbf{d} - \mathbf{S}_{SH}(\omega,\theta)V(\omega) &= \mathbf{f}(\omega) \\ i\omega\mathbf{S}_{SH}(\omega,\theta)\mathbf{d} + i\omega C_p^T V(\omega) &= I_c(\omega) \end{aligned} \tag{2}$$

where $\mathbf{S}_{SH}(\omega,\theta)$ is the shunt circuit spectral matrix, θ represents the variability, $\mathbf{d}$ is the generalized nodal displacement, $\mathbf{f}$ the generalized force. Similar to the nodal relationship of beam and beam-piezo elements, the behavior of the piezoelectric structure with the shunt circuit can be expressed with the equivalent nodal displacements and forces [4, 10]. Therefore, $\mathbf{S}_{SH}(\omega,\theta)$ can be assembled as follows

$$\mathbf{S}_{SH}(\omega,\theta) = [N_{e1}W(x_0,\omega), 0, -M_{e1}W(x_0,\omega), -N_{e2}W(x_0,\omega), 0, M_{e2}W(x_0,\omega)]^T \tag{3}$$

where

$$N_{e1} = N_{e2} = \frac{k_{ij}^2 i\omega Z^{EL} b_p d_{31} E_p}{1 + i\omega C_p^T Z_{eq}}, \qquad M_{e1} = M_{e2} = \frac{k_{ij}^2 i\omega Z^{EL} h b_p d_{31} E_p}{2 + 2i\omega C_p^T Z_{eq}}$$

The nodal functions of the piezoelectric structure with shunt circuit are related to the piezoelectric coupling coefficient k_{ij}, the width b_p, and the piezoelectric constant d_{31}. Therefore, a general representation of the dynamic behaviour of the unimorph beam is

$$\left[\mathbf{S}_{BP}(\omega) + \omega^2 \mathbf{S}_{SH}^2(\theta)\frac{1}{i\omega + 1/Z_{eq}(\theta)}\right]\mathbf{d}(\omega) = \mathbf{f}(\omega) \tag{4}$$

where $Z_{eq} = -V/I_c$ is the general impedance given by the junction of the admittance of the shunt circuit with the internal admittance of the piezoelectric. The impedance for open circuit and short circuit cases is presented with $Z_{eq} = i\omega C_P^T$ and $Z_{eq} = 0$, respectively. For the case of series resistive-inductive (RL) shunt circuit, also known as resonant shunt circuit, we have the following general impedance

$$Z_{eq} = \frac{R + i\omega L_n}{1 - \omega^2 L_n C_P^T + i\omega R C_P^T} \tag{5}$$

where R is the resistor and L_n is the inductor. For experimental practical purposes, the inductor component can be replaced by an antoniou circuit-type synthetic inductor (shown in Figure 2), and its tuning frequency ω_{SH} can be defined by

$$\omega_{SH} = \sqrt{\frac{1}{L_n C_P^T}} = \frac{1}{\sqrt{(C_1 R_1 R_3 R_4 / R_2) C_P^T}} \tag{6}$$

Once the matrices of the spectral elements $\mathbf{S}_B(\omega)$, $\mathbf{S}_{BP}(\omega)$ and $\mathbf{S}_{SH}(\omega)$ are defined, it is possible to obtain the global matrix by assembling the elements.

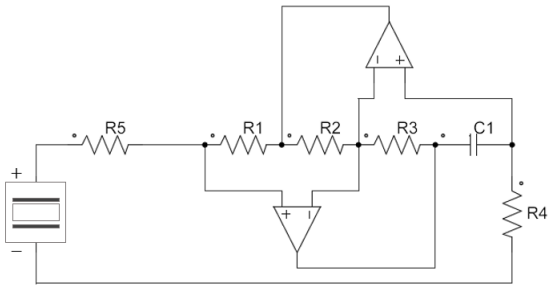

Fig. 2: Topography of a piezo connected in RL shunt circuit;

This procedure is similar to the one used in the Finite Element Method. Therefore, the global equation can be written so that

$$\mathbf{S}_g(\omega) = \mathbf{d}_g(\omega) = \mathbf{f}_g(\omega) \tag{7}$$

where $\mathbf{S}_g(\omega)$ is the assembled global dynamic stiffness matrix, $\mathbf{d}_g$ is the global spectral nodal DOFs vector, and $\mathbf{f}_g$ is the global spectral nodal forces and moments vector.

3 Numerical results and discurssion

The smart beam structure analyzed is an aluminum beam with seven piezoelectrics periodically coupled along the length L of the beam, as shown in Figure 3. The boundary condition used is free-free. A unit impulse is performed at the penultimate degree of freedom (driving point).

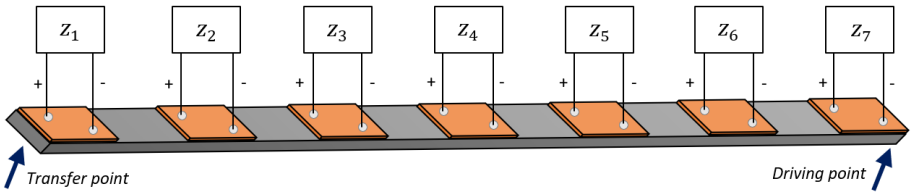

Fig. 3: Smart beam illustration.

The implementation of the structure model via SEM and TMM was performed using MatLab software. The properties and geometries considered for the beam are $E_b = 71GPa$, $\rho_b = 2700kg/m^3$, length $L = 0.5m$, width $12.7mm$ e thickness $h_b = 2.286mm$. For piezo were considered $E_p = 64.9GPa$, $\rho_b =$

$7600kg/m^3$, length $L = 38.46mm$, width $12.7mm$ e thickness $h_b = 0.762mm$. In addition, we considered the coupling coefficient $k_{31} = 0,31$, piezoelectric constant $d_{31} = -175\ m/Vx10^{-12}$, dielectric constant $\beta_{33}^S = -350\ m/Vx10^{-12}$ and piezoelectric capacitance $C_P^T = 200\ nF$ were considered. Regarding the resonant shunt circuits, the components $C_1 = 100\mu F$, $R_5 = 50\Omega$ and $R_1 = R_3 = R_4 = 1\ K\Omega$, were used for all circuits. However, different resistors R_2 with values 90, 103, 117, 132, 148, 165 and 182 Ω were used in each circuit to tune the frequencies 420, 450, 480, 510, 540, 570 and 600 Hz, respectively.

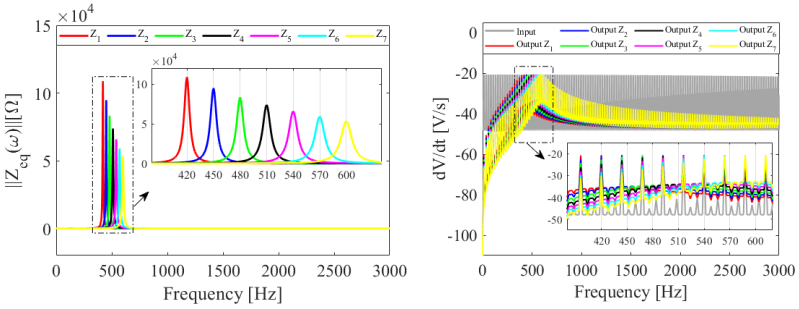

(a) (b)

Fig. 4: Electrical behavior of shunt circuits a) Impedance; b) Voltage.

Figure 4a shows the real part of the impedances of each resonant shunt circuit and Figure 4b shows the relationship between the voltage generated by the piezo and the voltage dissipated by each shunt circuit. These electrical relationships associated with each piezo coupled to the beam, result in the vibrational effect shown in Figure 5.

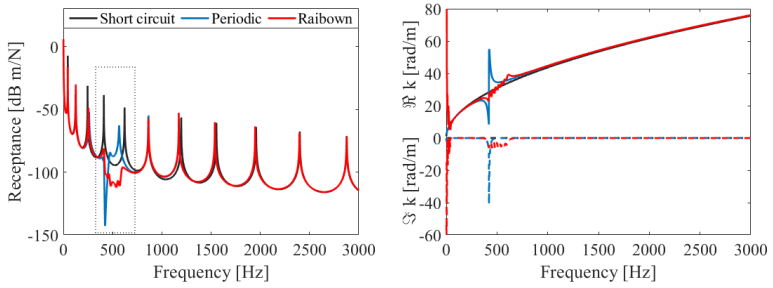

(a) (b)

Fig. 5: Vibrational comparison of the beam with 7 piezos connected in the short circuit, periodic and rainbow trap configurations: a) FRF; b) Dispersion diagram;

Figure 5a shows a vibrational comparison of Frequency Response Function (FRF) between the short circuit (black line), periodic impedance RL (blue line) and RL rainbow trap (red line) configurations. The same settings are used for wavenumber comparison in the dispersion diagram of Figure 5b.

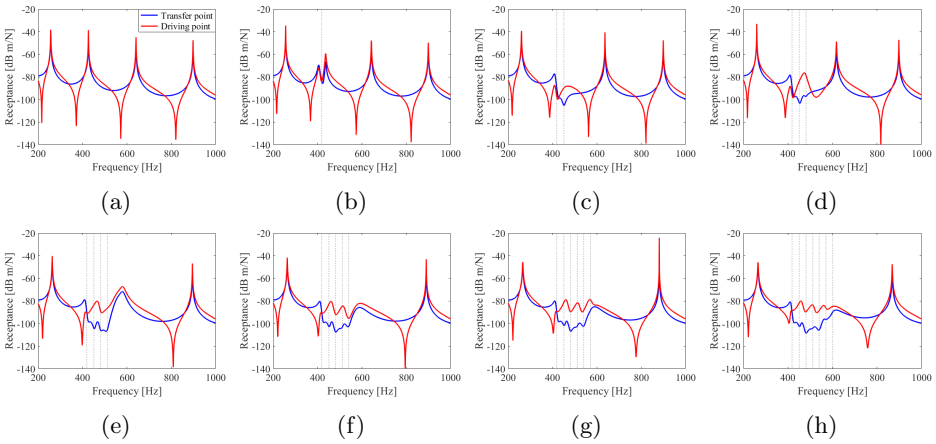

Fig. 6: Frequency response function of smart beam in rainbow trap setting; a) Short circuit; b) One connected shunt; c) Two connected shunt; d) Three connecteed shunt; e) Four connected shunt; f) Five connected shunt; g) Six coneected shunt; h) Seven connected shunt;

In Figure 6, the FRF is presented in the GDL where the forcing takes place (driving point) and in the opposite GDL where the forcing takes place (transfer point). In this analysis, all seven piezos are coupled along the beam, but the connection of the resonant shunt circuit happens in a restricted way in piezo to piezo. In Figure 6b, a resonant shunt circuit tuned at 420 Hz is connected to the first piezo. In Figure 6c a second resonant shunt circuit tuned at 450 Hz is connected to the second piezo. Likewise, in Figures 6d to 6h there is an addition of other resonant shunt circuits that are connected to each piezo, separately. However, each shunt circuit is tuned incrementally in 30 Hz until reaching 600 Hz.

Analyzing all the letters in Figure 6, it is observed a vibrational effect caused by the addition of each shunt circuit. This effect, known by the term band gap, is characterized by the creation of a vibration isolation band, and as a new resonant shunt circuit is added there is an increase in the band gap width. This effect can also be observed with the dispersion diagram in Figure 7.

In Figure 7 the dispersion diagram corresponding to the addition of resonant shunt circuits are presented. The yellow and green lines represent the positive and negative propagation waves corresponding to the transverse displacement, respectively. The red and blue lines represent the positive and negative prop-

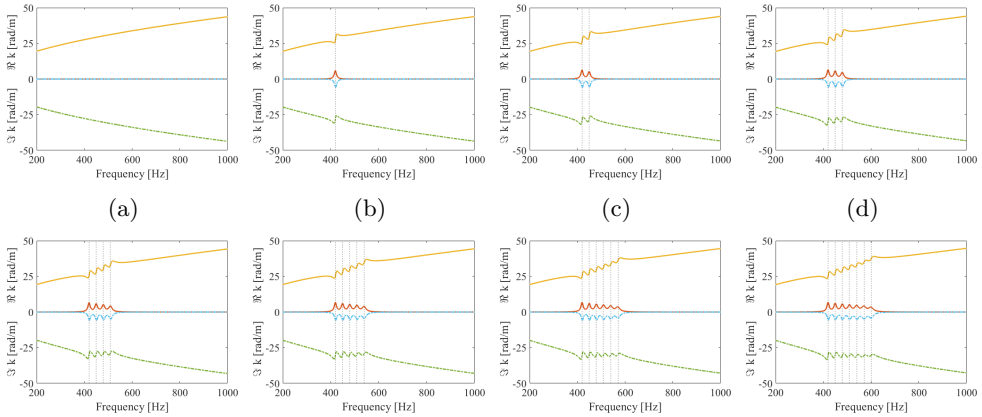

Fig. 7: Dispersion diagram of smart beam in rainbow trap setting; a) Short circuit; b) One connected shunt; c) Two connected shunt; d) Three connecteed shunt; e) Four connected shunt; f) Five connected shunt; g) Six coneected shunt; h) Seven connected shunt;

agation waves corresponding to the shunt circuit impedance, in that order. In all the figures it is possible to notice changes in the waves exactly in the tuning frequency.

4 Conclusion

This work approached an investigation on the band gap generation in a beam with seven piezoelectrics coupled in periodicity. A SEM and TMM model was used to implement the structure in MatLab software. A connection comparison of RL shunt circuits in short circuit, periodic impedance and rainbow trap configuration was performed to investigate band gap generation. With this, it was identified that the rainbow configuration is more susceptible to band gap generation. Furthermore, it was noticed that as new shunt circuits are added to the rainbow configuration, there is an increase in the isolation bandwidth (band gap). In summary, although these vibrational effects have already been explored in the literature, the present work demonstrated that the band gap width in the rainbow configuration can also be efficiently observed by the scatter diagram.

References

1. Airoldi, L., and Ruzzene, M.: Design of tunable acoustic metamaterials through periodic arrays of resonant shunted piezos. New Journal of Physics 13, Art. no. 113010, (2011).

2. Cardella, D., Celli, P., Gonella, S.: Manipulating waves by distiling frequencies: a tunable shunt-enabled rainbow trap. Smart Mater. Struct. **25**(085017), (2016).
3. Casadei F., Ruzzene M., Dozio L. and Cunefare K.: Broadband vibration control through periodic arrays of resonant shunts: experimental investigation on plates. Smart Mater. Struct., **19**(015002), (2009).
4. Doyle, J. F. Wave propagation in structures: a spectral analysis approach. 2. ed. New York: Springer-Verlag, (1997).
5. Gripp, J. A., and Rade, D. A.: Vibration and noise control using shunted piezoelectric transducers: A review. Mechanical Systems and Signal Processing, 112, 359–383 (2018).
6. Hagood, N. W., and Flotow, A. V.: Damping of Structural Vibrations With Piezoelectric Materials and Passive Electrical Networks, Journal of Sound and Vibration, **146**(2), 243-–268 (1991).
7. Hollkamp, J. J.: Multimodal passive vibration suppression with piezoelectric materials and resonant shunts. J. Intel. Mat. Syst Str. 5, 49—57 (1994).
8. Jaffe, B., Cook, R. and Jaffe, H.: Piezoelecfric ceramics. New York: Academic Press (1971).
9. Kaijun, Y., Matten, G., Ouisse, M., Sadoulet, E., Collet, M., and Chevallier, G.: Programmable metamaterials with digital synthetic impedance circuits for vibration control. Smart Materm Struct. **29**(035005), (2020).
10. Lee,U.: Spectral element method in structural dynamics. Singapore, Wiley, (2009).
11. Leo, D. J.: Engineering analysis of smart material systems. John Wiley & Sons, New Jersey, 1–7 (2007).
12. Machado, M. R., Fabro, A. T., and Moura, B. B.: Spectral element approach for flexural waves control in smart material beam with single and multiple resonant impedance shunt circuit. Journal of Computational and Nonlinear Dynamics, v. 1, 10.1115/1.4047389 (2020).
13. Sugino, C., Ruzzene, M., and Erturk,A.: Design and analysis of piezoelectric metamaterial beams with synthetic impedance shunt circuits, IEEE/ASME TRANSACTIONS ON MECHATRONICS, **23**(5), 2144–2155 (2018).
14. Uchino, K. and Ishii, T.: Mechanical damper using piezoelectric ceramics. Nippon Seramikkusu Kyokai Gakujutsu Ronbunshi/Journal of the Ceramic Society of Japan, **96**(8), 863–867 (1988).
15. Viana, F. A.; Steffen, J. V.: Multimodal vibration damping through piezoelectric patches and optimal resonant shunt circuits. Journal of the Brazilian Soc. of Mech. Sci. and Eng., 293—310 (2006).
16. Zhang, W., Cardella, D., and Gonella, S.: A disorder-based strategy for tunable, broadband wave attenuation. Proc. SPIE 10170, Health Monitoring of Structural and Biological Systems, 101700F (2017).
17. Wang, G., Cheng, J., Chen, J., and He, Y.: Multi-resonant piezoelectric shunting induced by digital controllers for subwavelength elastic wave attenuation in smart metamaterial. Smart Materials and Structures, **26**(2), (2017) .